Published in final edited form as:
Neuroscience. 2006 August 25; 141(2): 875–888. doi:10.1016/j.neuroscience.2006.04.035.

HISTOMETRIC CHANGES AND CELL DEATH IN THE THALAMUS AFTER NEONATAL NEOCORTICAL INJURY IN THE RAT

G. D. ROSEN[a,b,*,1], **B. MESPLES**[a,b], **M. HENDRIKS**[a,b], and **A. M. GALABURDA**[a,b,1]

[a]Dyslexia Research Laboratory and Charles A. Dana Research Institute, Department of Neurology, Division of Behavioral Neurology, Beth Israel Deaconess Medical Center, Boston, MA 02215, USA

[b]Harvard Medical School, Boston, MA 02115, USA

Abstract

Freezing injury to the developing cortical plate results in a neocortical malformation resembling four-layered microgyria. Previous work has demonstrated that following freezing injury to the somatosensory cortex, males (but not females) have more small and fewer large cells in the medial geniculate nucleus. In the first experiment, we examined the effects of induced microgyria to the somatosensory cortex on neuronal numbers, neuronal size, and nuclear volume of three sensory nuclei: ventrobasal complex, dorsal lateral geniculate nucleus, and medial geniculate nucleus. We found that there was a decrease in neuronal number and nuclear volume in ventrobasal complex of microgyric rats when compared with shams, whereas there were no differences in these variables in the dorsal lateral geniculate nucleus or medial geniculate nucleus. We also found that there were more small and fewer large neurons in both ventrobasal complex and medial geniculate nucleus. In experiment 2, we attempted to determine the role of cell death in the thalamus on these histometric measures. We found that cell death peaked within 24 h of the freezing injury and was concentrated mostly in ventrobasal complex. In addition, there was evidence of greater cell death in males at this age. Taken together, these results support the notion that males are more severely affected by early injury to the cerebral cortex than females.

Keywords

cell death; dorsal lateral geniculate nucleus; medial geniculate nucleus; microgyria; stereology; ventrobasal thalamus

Neuronal migration disorders of the cerebral cortex, such as heterotopias, microgyria, porencephaly, and lissencephaly, have been associated with a wide variety of disorders including intractable epilepsy (Meencke and Janz, 1984; Palmini et al., 1991a, b; Crino, 2004), dyslexia (Galaburda and Kemper, 1979; Galaburda et al., 1985), and developmental delay (Barkovich et al., 1988; Barkovich and Raybaud, 2004). Animal models have been

*Correspondence to: G. D. Rosen, Department of Neurology, Beth Israel Deaconess Medical Center, 330 Brookline Avenue, Boston, MA 02215, USA. Tel: +1-617-667-3252; fax: +1-617-667-5217. grosen@bidmc.harvard.edu (G. D. Rosen).
[1]These authors contributed equally to this work.

developed for many of these neuronal migration disorders. Some of these are the result of spontaneous genetic mutations, such as the *reeler* or *scrambler* mouse (Caviness et al., 1972; Goffinet, 1984; Sweet et al., 1996; D'Arcangelo et al., 1997; Rice et al., 1998) or the Tish rat (Lee et al., 1997; Chen et al., 2000), whereas others are induced in otherwise normal rodents such as by prenatal injection with methylazoxymethanol (Ferrer et al., 1982; Chevassus-au-Louis et al., 1999) or neurotrophin-4 (Brunstrom et al., 1997).

Malformations have also been induced by mechanical disturbances of the cortical plate. Thus, focal collections of neurons in the molecular layer can be induced by puncture wounds at or around birth (Rosen et al., 1992b), and freezing injury to the developing cortical plate induces malformations that resemble human four-layered microgyria (Dvorák and Feit, 1977; Dvorák et al., 1978; Humphreys et al., 1991; Rosen et al., 1992a; Ferrer et al., 1993; Marret et al., 1995). These induced malformations have been used to model a variety of disorders, including epilepsy (Luhmann et al., 1998; Chevassus-au-Louis et al., 1999; Jacobs et al., 1999a; Jacobs and Prince, 2005) and developmental dyslexia (Humphreys et al., 1991; Fitch et al., 1994, 1997a; Herman et al., 1997; Rosen et al., 1999; Peiffer et al., 2004).

The effects of these relatively small focal malformations extend beyond the obvious distortion of the cerebral cortex. Recordings from slices of cortex containing microgyria induced by freezing injury to the cortical plate, for example, reveal epileptogenic discharges as far as 2–4 mm away from the malformation (Jacobs et al., 1996, 2000; Luhmann and Raabe, 1996; Jacobs and Prince, 2005). Using the same model, we and others have demonstrated a variety of connectional, anatomic, and behavioral alterations associated with the presence of this type of malformation. For example, both cortico-cortical and thalamo-cortical connections are disturbed not only in the malformation itself, but in areas both proximal and distal to it (Giannetti et al., 1999, 2000; Rosen et al., 2000). Anatomically, induction of microgyria dramatically decreases brain weight and neocortical volume globally (Peiffer et al., 2003). Microgyria in the somatosensory cortex not only disrupts the formation of barrel fields in that hemisphere (Jacobs et al., 1999b), but also distorts the barrel field of the opposite hemisphere (Rosen et al., 2001). Behaviorally, we have reported that adult and young male subjects with induced microgyria have defects in rapid auditory processing—a defect also seen in many individuals with language impairment and developmental dyslexia (Tallal and Piercy, 1974; Fitch et al., 1997b)—when compared with controls with no malformations. In comparison, adult females with identical malformations have no difficulty in processing this type of stimuli (Fitch et al., 1994; Clark et al., 2000a; Peiffer et al., 2004).

Because studies of the brains of individuals with developmental dyslexia had exhibited changes in cell size in the medial geniculate nucleus (MGN) and dorsal lateral geniculate nucleus (dLGN) of the thalamus (Livingstone et al., 1991; Galaburda et al., 1994), we measured cell size in these two nuclei in male and female rats with and without induced microgyria (Herman et al., 1997). We found more small and fewer large neurons in the MGN of male microgyrics when compared with their sham littermates. There was no difference between microgyrics and shams in the females. In addition, there were no differences in cell size distribution among any of the groups in the dLGN. We further reported that the difference in the MGN resulted from perinatal effects of gonadal hormones

—female microgyrics exposed to testosterone in the perinatal period had cell size distributions in the MGN similar to those of males (Rosen et al., 1999).

These findings raise a number of questions. We have established that damage to neonatal somatosensory cortex changes cell size distribution in a thalamic nucleus to which it is not connected, at least during adulthood. What is not yet known is how these changes compare with those in thalamic nuclei directly connected to the area of injury. Moreover, what effects might be seen in other thalamic nuclei that do not connect with the somatosensory cortex? By what process are these changes in thalamic cell size distribution occurring? Is cell death affecting one neuronal population more than another, or could differences in cell proliferation, whereby one cell type is affected out of proportion to others, underlie these differences? In the present study, we first focused on stereologically assessing histometric features in the thalamus following early somatosensory cortical freezing injury. We examined effects in a directly connected thalamic nucleus (the ventrobasal complex (VB)), a nucleus that receives transient developmental connections from the somatosensory cortex (MGN, Nicolelis et al., 1991), and a nucleus that never connects directly with the somatosensory cortex under normal conditions (the dLGN). We then examined the patterns of cell death throughout the thalamus following freezing injury to the developing cortical plate in an effort to determine the contribution of this variable to the histometric changes.

EXPERIMENTAL PROCEDURES

Two experiments were conducted in this study. Experiment 1 investigated changes in neuron number, neuron size, and regional volume in three thalamic nuclei following postnatal freezing injury to the somatosensory neocortex. Experiment 2 investigated cell death in the thalamus following postnatal freezing injury to the somatosensory cortex. All procedures involving animal care and experimentation were carried out in accordance with guidelines provided by the National Institutes of Health and approved by the institutional animal care committee at Beth Israel Deaconess Medical Center. Care was taken to minimize the number of animals used, as well as their pain and suffering.

Experiment 1 protocol

On postnatal day (P) 1, rats were randomly assigned to receive freezing injury to the cerebral cortex or to a sham surgery. In adulthood, the subjects were killed, their brains removed, embedded in celloidin, sliced in the coronal plane, stained with Cresyl Violet, and every 5th section mounted on glass slides. Using stereologic probes, we estimated the number of neurons, the sizes of neurons, and the volume of VB, MGN, and dLGN nuclei.

Subjects

A subset of 24 subjects (six male lesioned, six male shams, six female lesioned, and six shams) was randomly chosen from subjects of a previous experiment and prepared as described previously (Rosen et al., 1999). In brief, timed pregnant rats were obtained from Charles River Laboratory (Wilmington, MA, USA) in the last week of gestation. The pregnant females were singly housed under a 12-h light/dark cycle and were provided with food and water *ad libitum*. On P1, male and female pups were randomly assigned either to

receive bilateral freezing injury to the somatosensory cortex or to a sham condition. Subjects were anesthetized by placement on ice for 2 min. A small incision on the scalp was made midsagittally. For those subjects receiving freezing lesions, a cooled (−70 °C) probe was placed over the presumptive somatosensory cortex (directly on bregma, approximately 2 mm medial to the sagittal suture) for 5 s. The procedure was repeated on the opposite hemisphere with a second cooled probe. Animals receiving sham surgery were treated identically, with the exception that the probe was at room temperature. The incision was sutured, ink was injected into the footpads for identification, and the pups were warmed before being returned to their mother.

At P70–100, the subjects were deeply anesthetized (xylazine/ketamine 100 mg/ml) and killed by transcardial perfusion with 0.9% saline followed by 10% formalin. The brains were removed from the skull and allowed to post-fix for at least one week prior to embedding. Afterward, the brains were dehydrated in graded ethanols and embedded in 12% celloidin. They were then cut in the coronal plane at 30 μm, stained with Cresyl Violet, and every 5th section was mounted on glass slides with Permount.

Stereological measures

All stereological measures were performed using Stereo Investigator (MBF Bioscience, Williston, VT, USA). Experimenters were blinded with respect to sex and treatment. Neuron numbers within each thalamic nucleus were estimated using the optical fractionator probe, and neuron sizes were determined concurrently with the nucleator probe. Volumes of the thalamic nuclei were determined with point counting using Cavalieri's rule. In cases where there were missing or damaged sections, a piece-wise parabolic estimation was used (Rosen and Harry, 1990). The parameters for these probes for each of the thalamic nuclei are shown in Table 1. Section thickness, which ranged from 25 to 36 μm, was measured every eight sections, and this value was used in all computations.

The borders of the thalamic nuclei were determined using a standard stereotaxic atlas as a guide (Paxinos and Watson, 1986). The ventroposterolateral (VPL) and ventroposteromedial (VPM) nuclei composed the VB complex in this study, and the MGN measurements included all its subdivisions (the medial, lateral, and dorsal; Fig. 1). Neurons were distinguished from glial cells by the presence of a single distinct nucleolus in the nucleus. In order to be counted, neurons had to be in focus within the disector depth and contained within the active borders of the counting frame.

Histologic analysis

Nissl-stained sections were examined under a Zeiss Axiophot (Carl Zeiss MicroImaging, Inc., Thornwood, NY, USA) light microscope with a Ludl Mac5000 motorized stage (Ludl Electronic Products Ltd., Hawthorne, NY, USA) interfaced to a Dell OPTIPLEX GX260 computer (Dell Computers, Austin, TX, USA) to define the localization of the lesion. Neurolucida (MBF Bioscience) was used to trace the cortical pial surface from the serial sections, and lesion localization was visualized by placement onto a flattened map of the cerebral cortex derived from Zilles (1985), as described previously (Herman et al., 1997).

Volume of microgyria was estimated in Stereo Investigator using point counting and Cavalieri's rule.

Statistical analysis

Data were analyzed using ANOVA, regression, and chi-square techniques on an Apple Macintosh G4 (Apple Computer, Cupertino, CA, USA) computer using standard statistical software (JMP and StatView, SAS Institute, Cary, NC, USA).

Protocol experiment 2

We obtained time-mated pregnant Wistar rats from Charles River Laboratories. The pregnant females were singly housed under a 12-h light/dark cycle and were provided with food and water *ad libitum*. On the day of birth, the male and female pups from these subjects were assigned to receive either freezing injury to the somatosensory cortex (see below) or sham surgery. The pups were subsequently killed by transcardial perfusion with saline followed by 4% paraformaldehyde (PFA) at 8, 24, 72, 120, and 168 h after surgery. The brains were removed, embedded in paraffin, and adjacent series of sections processed for markers of cell death (TUNEL (terminal deoxynucleotidyl transferase-mediated dUTP-biotin nick-end labeling), Fluoro-Jade B (FJB)) or with Thionin for Nissl substance. The distribution and number of degenerating and apoptotic cells in the thalamus were recorded for each of the subjects. A summary of the number of subjects in this experiment can be found in Table 2.

Induction of microgyria

Microgyria were induced in the right somatosensory cortex identically to experiment 1 with the exception of the duration, which was either 5 or 10 s. Animals from the control group received sham surgery. Following treatment, the skin was rapidly sutured and subjects marked with ink footpad injections, warmed under a lamp, and returned to the mother.

Perfusion

Subjects were deeply anesthetized as described for experiment protocol 1 and perfused with 0.9% saline followed by cold 4% PFA. Brains were quickly removed and post-fixed overnight in the same fixative.

Histology

Paraffin embedding—Post-fixed brains stayed for 3 days in 70% alcohol before being gradually dehydrated in graded ethanol and then immersed in xylene baths for several hours in an automatic processing machine. The brains were immersed in two changes of paraffin, oriented along the anterior–posterior axis, and embedded in a histological cassette. They were then sliced at 10 μm on a rotary microtome, and six series of every 20th section were mounted onto glass slides.

Nissl staining—Sections were deparaffinized in xylene, hydrated through graded ethanol, rinsed in dH_2O for 2 min before being immersed in 0.05% Thionin for 30 min. Sections were dehydrated, cleared in xylene, mounted and coverslipped with Permount.

FJB—FJB stains for degenerating neurons (Schmued et al., 1997). Sections were deparaffinized in three changes of xylene for 15 min each and hydrated through 100% ethanol for 5 min before being placed in 1% NaOH/ethanol solution for 5 min. This was followed by 2 min in 70% ethanol. Sections were then rinsed in dH2O for 2 min and agitated on a shaker in 0.06% $KMnO_4$ for 10 min. The sections were then rinsed in dH2O and stained in FJB working solution (0.004%) for 20 min. Sections were rinsed in dH_2O, dried, cleared in xylene, mounted and coverslipped with DPX mounting media. When the slides were dry, they were sealed with Permount.

TUNEL—TUNEL stains for cells dying through mainly apoptotic mechanisms (Gavrieli et al., 1992). Sections were deparaffinized in three changes of xylene for 15 min each. Sections were then hydrated through graded alcohols and dH_2O over 15 min. The sections were placed in proteinase K (20 μg/ml) in 10 mM Tris-HCl pH 7.4 for 20 min at 37 °C. Sections were rinsed in two changes of phosphate-buffered saline (PBS) before being placed in a permeabilization solution (Triton 100X 1% in 0.1% potassium citrate) for 2 min at 4 °C. After two PBS washes, the TdT+kit (F. Hoffmann-La Roche Ltd., Basel, Switzerland) buffer mixture (1 μl of enzyme for 9 μl of nucleotides buffer) was placed on the slide (150 –250 μl/slide), which then incubated at 37 °C for 1 h. The slides were then washed in PBS, dehydrated through dH_2O and graded alcohols, cleared in xylene and mounted with DPX mounting media. When the slides were dry, they were sealed with Permount.

Analysis—Nissl-stained sections were examined as described above (see *Histologic Analysis*), and lesion location at each age was plotted on a flattened map of the cortex. Volume of microgyria was estimated in Stereo Investigator using point counting and Cavalieri's rule. The contour of sections cut at the level of the thalamus was drawn using Neurolucida, after visualizing the sections with a Microfire (Optronics Inc., Goleta, CA, USA) digital camera. These contours were subsequently aligned to the FJB-and TUNEL-stained slides to define the localization of the stained cells.

FJB- and TUNEL-stained sections were examined under fluorescence throughout the entire extent of the thalamus. FJB also stains vascular elements (Schmued et al., 1997). These cells differed in brightness and structure and were ignored. FJB-positive profiles were counted throughout the thalamus, and their positions charted using Neurolucida. Experimenters were blind with respect to sex and treatment. To assess reliability, a second observer recounted six brains.

Statistical analysis

Data were analyzed using ANOVA and multiple regression techniques on a Macintosh PPC computer using JMP and StatView as described under experiment protocol 1.

Image manipulations

Photomicrographs were adjusted for exposure and sharpened (unsharp mask filter) using Adobe Photoshop (Adobe Inc., San Jose, CA, USA). Image montages were created in Canvas X (ACD Systems, Miami, FL, USA).

RESULTS

Experiment 1

Histology—As expected, freezing injury to the developing cortical plate resulted in a malformation resembling four-layered microgyria (Dvorák et al., 1978; Humphreys et al., 1991; Rosen et al., 1992a, see Fig. 2A). These malformations were located predominantly in the somatosensory cortex, including Par1, HL, and FL (Fig. 2B). There was no evidence of neocortical damage in the sham subjects. There were no differences in lesion size between males and females (mean±S.E.M.=19.1±2.7 mm^3 vs. 17.7±2.2 mm^3, respectively, $t<1$, ns).

There is a decrease in neuron number in the VB complex—The results of the estimates of neuron number are summarized in Fig. 3. The coefficient of error for the optical fractionator estimation of neuron number for all nuclei ranged from 0.06–.12 and averaged 0.085. In VB, an ANOVA with Sex (male vs. female) and Treatment (microgyria vs. sham) as independent measures and neuron number as the dependent measure revealed a significant effect of treatment ($F_{1,20}=26.5$, $P<0.001$). Examination of the means indicated that there was a decrease of about 28% in neuron numbers in the subjects with microgyria when compared with shams. There was no main effect of Sex ($F_{1,20}<1$, ns), nor was there any interaction between Sex and Treatment ($F_{1,20}<1$, ns) indicating that this decrease in lesioned subjects was similar for males and females (Fig. 3A). In contrast, there were no differences in neuron number in either the MGN or dLGN (see Fig. 3A), and there were no significant main effects or interactions for either of the dependent variables in either of these two nuclei.

The volume of VB is decreased in subjects with microgyria—The results of the estimation of volume of the thalamic nuclei are summarized in Fig. 3B. The coefficient of error for estimating volume using Cavalieri's rule ranged from 0.026 –.058 for all nuclei and averaged 0.038. In VB, an ANOVA with Sex and Treatment as independent variables and regional volume as the dependent measure revealed a significant effect of Treatment ($F_{1,20}=14.3$, $P<0.01$) and no other main effects or interactions ($F_{1,20}<1$, ns in both cases). The volume of VB in subjects with microgyria was, on the average, 25% less than that of shams. In contrast, there were no differences in the volumes of MGN or dLGN between microgyric and sham subjects.

Sexually dimorphic differences in cell size in VB and MGN, but not in dLGN—In previous work, we failed to demonstrate significant differences in mean neuronal size in the MGN between treatment groups. Instead, we demonstrated differences in the distribution of neuron sizes. As expected, therefore, ANOVA with Sex and Treatment as independent variables and neuron size as the dependent measure did not reveal any significant main effects or interactions in either VB or dLGN. We did, however, find a significant effect of Treatment ($F_{1,20}=7.1$, $P<0.05$) and a Sex times]Treatment interaction ($F_{1,20}=6.8$, $P<0.05$) in the MGN (Fig. 4).

To determine the neuron size distribution, we placed adjacent ranges of neuronal sizes into bins for each group and performed a chi-square analysis. As in previous work, we set a highly conservative αlevel (0.0001) to reject the null hypothesis. In VB, there were more

small and fewer large cells in males with microgyria as compared with shams (χ^2=55.3, *df*=13, *P*<0.0001). In females, there were no significant differences between the microgyric and sham subjects (χ^2=27.6, *df*=13, ns; Fig. 5A). This same sexually dimorphic pattern was seen in the MGN, with microgyric males having more small and fewer large neurons than shams (χ^2=199.1, *df*=13, *P*<0.0001), whereas there were no significant differences within females (χ^2=28.8, *df*=13, ns; Fig. 5B). In the dLGN, no significant differences were seen between microgyric and sham subjects in either males (χ^2=27.7, *df*=13, ns) or females (χ^2=37.6, *df*=13, ns; Fig. 5C).

Experiment 2

Experiment 1 suggested that freezing injury to the somatosensory cortex results in decreased volume and neuron numbers in VB, but not in MGN or dLGN. However, such injury does lead to differences in cell size distribution, which is sexually dimorphic, in both the MGN and the VB complex. In experiment 2, we sought to determine whether thalamic cell death following freezing injury to the presumptive somatosensory cortex contributed to these findings.

Histology

As expected, there was no evidence of damage in sham-operated subjects. We assessed the extent of damage of the brains taken from subjects killed at 8, 24, and 72 h after the freezing injury (Fig. 6). As has been reported previously (Rosen et al., 1992a; Rosen and Galaburda, 2000), freezing injury to the developing cortical plate results in a distinct area of necrosis that kills the underlying neurons. This is apparent in the subjects killed both 8 and 24 h after the freezing injury. By 72 h, the extent of the necrotic area has decreased, and the beginnings of the formation of the microgyric region can be seen.

We plotted the location of the damaged regions on flattened maps of the neocortex, and found no differences in the region of cortical destruction between males and females at any age (Fig. 7). As expected, there was a greater percentage of cortical plate damaged in the 8 h subjects than in those killed at 72 h, because of subsequent brain growth. There was no difference in the volume of microgyria between males and females at 8 h (mean ±S.E.M.=3.02±0.27 mm^3 vs. 3.14±0.33 mm^3, respectively, $F_{1,7}$<1, NS), 24 h (mean ±S.E.M.=2.32±0.28 mm^3 vs. 2.05±0.17 mm^3, respectively, $F_{1,20}$<1, NS), and 72 h (mean ±S.E.M.=1.61±0.16 mm^3 vs. 1.67±0.19 mm^3, respectively, $F_{1,23}$<1, NS).

Cell death in the thalamus and cortex occurs within 72 h after injury

Gross examination of the TUNEL- and FJB-stained sections revealed that there were few, if any, TUNEL- or FJB-positive profiles in subjects killed 120 and 168 h after freezing injury. These 10 subjects comprising this time period were excluded from the analysis. The somatosensory cortex and the thalamus of the remaining subjects were surveyed for the presence of FJB- and TUNEL-stained cells. As expected, there was little TUNEL or FJB-positive staining in the sham subjects. Examination of animals with freezing injury revealed dense regions of TUNEL- and FJB-positive profiles in the lesioned somatosensory cortex (Fig. 7A, B). In contrast, there were relatively few TUNEL-positive profiles in the thalamus at any of the ages examined, whereas intense FJB-positive staining was observed (Fig. 7C,

D). The lack of TUNEL-positive profiles indicated that there was relatively little apoptotic cell death in the thalamus, and suggested that the overwhelming majority of cell death in the thalamus was the result of degeneration. We therefore only counted FJB-positive profiles in the thalamus, thereby deriving a relative measure of both apoptotic and degenerative cell death.

Most dying cells in the thalamus are located in VB

We counted the number of FJB-positive profiles throughout the thalamus in both lesioned and sham subjects. There were two distinct types of FJB-positive profiles observed in the thalamus: large (≥10 μm diameter) and small (≤3 μm diameter); see Fig. 8A). We cannot determine exactly what these different size profiles represent, but because they may represent differential aspects of neuronal cell body or neuropil degeneration, they were counted separately. Thus, for each subject the numbers of large and small profiles were recorded (Fig. 8B).

Of the lesioned brains, there were two female subjects killed at 24 h that had no FJB-positive profiles in the thalamus, and they were removed from the analysis, leaving 53 lesioned subjects. Surveying the thalamus of these lesioned brains revealed that each subject had large numbers of FJB-positive profiles in VB. In contrast, there were only six subjects with FJB-positive profiles outside of this nucleus. These profiles were located in the MGN (two subjects), lateral posterior nucleus (four subjects), dLGN (two subjects), and one subject each in laterodorsal, reticular, and anteroventral nuclei (some subjects had FJB-positive profiles in more than one nucleus). As a result, we only quantified the number of FJB-positive profiles in VB. The numbers of FJB-labeled profiles in VB were counted in six subjects by two investigators. The results were within 10% of one another, and the reliability coefficient was 0.91.

There is an increase in FJB-positive profiles in the VB complex of subjects with microgyria

The mean numbers of FJB-positive cells in male and female lesioned and sham subjects (irrespective of age of kill) are summarized in Table 3. We performed a series of ANOVAs with Treatment (Sham vs. Microgyria) and Sex as independent measures and the number of large and small FJB-positive profiles as dependent measures. There was a significant effect of Treatment for large and small FJB-positive profiles ($F_{1,57}$=4.4, P<0.05; $F_{1,57}$=7.7, P<0.01, respectively), with the number of profiles an order of magnitude greater in subjects with freezing lesions as compared with sham subjects. There were no main effects of Sex, nor any Sex×Treatment interactions for any of the dependent measures.

There are significant effects of age and sex on the number of FJB-positive profiles

To examine the effects of sex and age of kill in the lesioned subjects, we performed additional ANOVAs with Sex and Age (8 h, 24 h, and 72 h) as independent measures and the number of profiles (large, small, and total) as dependent measures. There were no significant effects of Age ($F_{2,47}$=2.1, ns), Sex ($F_{2,47}$<1, ns) or their interaction ($F_{2,47}$=1.1, ns) for large FJB-positive profiles (Fig. 9A). In contrast, there was a significant main effect of Age in the number of small profiles ($F_{2,47}$=7.6, P<0.01). Post hoc tests indicated that there were significantly more small profiles at 24 h than at either 8 h or 72 h post-injury

(Fisher PLSD, $P<0.01$; Fig. 9B). There was also a main effect of Sex for this dependent measure ($F_{1,47}=4.1$, $P<0.05$). Post hoc analysis one-way ANOVAs at each age indicated a significant Sex effect only at 24 h ($F_{1,19}=5.6$, $P<0.05$), with males having significantly greater numbers of small profiles than females. There was no significant Sex×Age interaction ($F_{2,47}=2.1$, ns).

DISCUSSION

There are differential effects on sensory nuclei of the thalamus following freezing injury in the first day of life to the presumptive somatosensory cortex of the rat. In the directly connected VB, there is a significant decrease in neuron number as well as nuclear volume in the male and female subjects with lesions when compared with shams. In contrast, there were no changes in lesioned subjects in neuron numbers or nuclear volume in MGN or dLGN, the other two sensory thalamic nuclei examined. Both VB and MGN showed sexually dimorphic alterations of cell size distribution: There were more small and fewer large cells in male subjects with microgyria as compared with sham littermates. This difference was not apparent in the dLGN, nor was it seen in females in any of the three nuclei.

Examination of the patterns of cell death in the thalamus following early damage to the presumptive somatosensory cortex using FJB revealed that the overwhelming majority of necrotic cell death in the thalamus occurs in VB. The number of FJB-positive profiles peaked at 24 h after the injury, and there were no FJB-positive profiles in the thalamus after 72 h. There was an intriguing sex difference in the number of small profiles in the 24 h group, with females having significantly fewer FJB-positive profiles than males. The best interpretation of this finding is that large neurons are dying out of proportion in males compared with females.

Neuron numbers in the thalamus

The optical fractionator probe provides accurate and unbiased estimates of cell number (Gundersen, 1986; Gundersen et al., 1988), and the coefficients of error computed in the present study support this contention. The numbers of neurons in the MGN and dLGN match those from our previously published data (Herman et al., 1997), which employed 3-D counting instead of an optical fractionator (Williams and Rakic, 1988). There are surprisingly few studies that have used unbiased stereology to examine cell number and volume in the thalamus for comparison to the current results. As part of a larger study on subcortical auditory nuclei in rats, the number of neurons in the MGN was measured by Kulesza et al. (2002). They reported an average of 72,000 neurons in the MGN of female rats, which is fewer than what we report here (~110,000). The number of neurons in the dLGN has been estimated to be around 40,000 (Diaz et al., 1999), which again is smaller than the numbers we have obtained (~75,000). Stereological estimation of the number of neurons in VB has yet to be reported, although Luczynska et al. (2003) estimated the number of neurons in VPL to be approximately 14,000 in adult rat.

There are methodological differences that prevent direct comparison between the results reported here and those previously published. In the case of the MGN and VPL, the

investigators based their estimations on frozen sections, which are not optimal for the optical fractionator due to nonuniform compression of cells in the *z* axis (Gardella et al., 2003) and are inferior to celloidin-embedded sections for that reason. In the case of the dLGN, it is unclear whether the investigators estimated neurons from both hemispheres in their paraffin-embedded sections. In addition, these investigators did not employ an optical fractionator and their results cannot be considered unbiased. Validation of the numbers derived in this study, therefore, awaits replication using comparable probes and material.

In previous work, we have examined issues related to neuron number and size in the MGN and LGN following injury to the somatosensory cortex. Although there is no difference in neuron numbers in MGN between lesioned and sham subjects, we have repeatedly found more small and fewer large neurons in the MGN of male, but not female, subjects sustaining a freezing injury to the somatosensory cortex (Herman et al., 1997; Rosen et al., 1999; Peiffer et al., 2002). We have also demonstrated that there is no difference in the volume of the MGN between lesioned and sham subjects. That the results of the current study replicate these previous results is not surprising given that the subjects used here are a randomly chosen subset of those used in one of the previous studies (Rosen et al., 1999). In this study, however, we used strict unbiased stereologic principles to both estimate neuron number and measure neuron size, which increases confidence in the results. Previously published results on the effects of microgyria on the dLGN are also replicated in the current experiment (Herman et al., 1997) with a completely independent set of subjects.

The morphometric results in VB in the current experiment are reported for the first time. Unlike the MGN and LGN, there is a significant decrease in neuron numbers in both sexes. This is not a surprising result, as VB has direct connections to the somatosensory cortex, and loss of cells in this nucleus due to axonal damage and resultant retrograde degeneration is expected. Similarly, the significant decrease in VB volume is not surprising. We have seen a similar decrease in nuclear volume and neuron numbers in the dLGN following freezing injury to the occipital cortex (Herman et al., 1997).

What was unexpected, however, was the sexually dimorphic change in cell size distribution in VB that is identical to that seen in the MGN. In both thalamic nuclei, male subjects with freezing injury to the somatosensory cortex have more small and fewer large cells than their sham counterparts, whereas there is no difference among females. These results suggest that changes in neuron size distribution are dissociable from those in neuron number and nuclear volume, whereby the former is seen in both VB and MGN, and the latter is seen only in VB. Thus, it would appear unlikely that the same degenerative mechanisms that decrease neuron number and nuclear volume are also responsible for the changes in neuron size distribution. This conclusion is supported by pattern of cell death in the MGN following early injury to the neocortex.

The role of cell death in the thalamus following early injury to the cortex

Surveying the thalamus for FJB-positive profiles in the period after early freezing injury to the presumptive somatosensory cortex of the rat reveals that the overwhelming majority of profiles are located in VB. Evidence of degeneration in the thalamus peaks within 24 h of the injury, and decreases to background levels 4 days later. When small profiles are

considered, we find intriguing sex differences, with males having a greater number of profiles than females 24 h after injury. In order to interpret these results, however, it is necessary to consider what the distinct profiles we measured may indicate.

FJB is a marker of both apoptotic and necrotic degenerating neurons in the CNS, although its precise mechanism of action is not known. FJB-positive activity can be seen in all aspects of degenerating neurons, including cells bodies, dendrites, axons, and terminals and does not label glial cells in the CNS (Schmued et al., 1997). We determined that FJB-positive profiles could be grouped into two distinct categories: large and small profiles. “Large” profiles most likely represent degenerating neuronal cell bodies, while “small” profiles are likely degenerating neuropil. We did not see significant effects of Age or Sex in the large profiles, although there was a trend ($F_{1,19}$=3.9, P=0.062) to more large profiles in males at 24 h, but there were significant effects of Age and Sex in the number of small profiles. Taken together, we interpret these findings to mean a greater loss of large neurons in males than females.

Alternatively, it could be that there is a difference in the rate of clearance between the sexes. In this case, the increase in the number of small profiles by the males would be indicative not of greater large cell death in males but rather of a faster clearance of degenerating neurons in females. In previous work, although there were macrophages present 24 h after the injury, the heaviest concentration of macrophage activity did not occur until 48 h later (Humphreys et al., 1991). Moreover, we did not note any sex differences in macrophage activity at either of these ages. However, the present study did not assess macrophage activity, and, although we consider clearance differences unlikely, we cannot exclude that possibility.

Sexually dimorphic effects of early injury

There are a variety of sex differences in the response of the thalamus to early injury to the cerebral cortex. We have previously reported that there are more small and fewer large neurons in the MGN of male, but not female, subjects with freezing injury of the developing cortical plate (Rosen et al., 1997, 1999; Peiffer et al., 2002). In the current experiment we have extended these results to include the VB nucleus. We have previously reported that male rats with induced microgyria have defects in rapid auditory processing (Fitch et al., 1994, 1997a; Clark et al., 2000a,b; Peiffer et al., 2001, 2003, 2004), suggesting that these changes in the thalamus have functional consequences. In the current experiment, we report that there are significantly more FJB-positive profiles in VB at 24 h in males when compared with females. What is important to emphasize in all these cases is that the extent of cortical damage is identical between male and female. This suggests that the female thalamus is better protected against the effects of early damage.

There is evidence from the human literature to suggest that the consequences of perinatal brain injury are more severe in males than in females. For example, Raz et al. (1995) examined the cognitive abilities of boys and girls who had sustained similar perinatal intracranial hemorrhages, and found that males were more severely impaired. Similar data were reported for infants with respiratory distress syndrome when examined between 5 and 6 years of age (Lauterbach et al., 2001). In this case, females had a significant cognitive

advantage over males, especially in non-verbal tasks. There is also a significant male–female difference in the cognitive ability of extremely low birth weight infants at 2 years of age, with females having less cognitive impairment (Hindmarsh et al., 2000). Taken together, these results support the contention that the male brain responds more poorly to early injury than the female brain.

Acknowledgments

This work was supported, in part, by NIH grant HD20806. The authors wish to acknowledge the expert technical assistance of Karen Heindl.

Abbreviations

dLGN	dorsal lateral geniculate nucleus
FJB	Fluoro-Jade B
MGN	medial geniculate nucleus
P	postnatal day
PBS	phosphate-buffered saline
PFA	paraformaldehyde
TUNEL	terminal deoxynucleotidyl transferase-mediated dUTP-biotin nick-end labeling
VB	ventrobasal complex
VPL	ventroposterolateral nucleus of the thalamus

References

Barkovich AJ, Chuang SH, Norman D. MR of neuronal migration anomalies. Am J Roentgenol. 1988; 150:179–187. [PubMed: 3257118]

Barkovich AJ, Raybaud CA. Neuroimaging in disorders of cortical development. Neuroimaging Clin N Am. 2004; 14:231–254. viii. [PubMed: 15182817]

Brunstrom JE, Gray-Swain MR, Osborne PA, Pearlman AL. Neuronal heterotopias in the developing cerebral cortex produced by neurotrophin-4. Neuron. 1997; 18:505–517. [PubMed: 9115743]

Caviness VS Jr, So DK, Sidman RL. The hybrid reeler mouse. J Hered. 1972; 63:241–246. [PubMed: 4644329]

Chen ZF, Schottler F, Bertram E, Gall CM, Anzivino MJ, Lee KS. Distribution and initiation of seizure activity in a rat brain with subcortical band heterotopia. Epilepsia. 2000; 41:493–501. [PubMed: 10802753]

Chevassus-au-Louis N, Baraban SC, Gaiarsa JL, Ben-Ari Y. Cortical malformations and epilepsy: new insights from animal models. Epilepsia. 1999; 40:811–821. [PubMed: 10403203]

Clark MG, Rosen GD, Tallal P, Fitch RH. Impaired processing of complex auditory stimuli in rats with induced cerebrocortical microgyria: An animal model of developmental language disabilities. J Cogn Neurosci. 2000a; 12:828–839. [PubMed: 11054924]

Clark MG, Rosen GD, Tallal P, Fitch RH. Impaired two-tone processing at rapid rates in male rats with induced microgyria. Brain Res. 2000b; 871:94–97. [PubMed: 10882787]

Crino PB. Malformations of cortical development: molecular pathogenesis and experimental strategies. Adv Exp Med Biol. 2004; 548:175–191. [PubMed: 15250594]

D'Arcangelo G, Nakajima K, Miyata T, Ogawa M, Mikoshiba K, Curran T. Reelin is a secreted glycoprotein recognized by the CR-50 monoclonal antibody. J Neurosci. 1997; 17:23–31. [PubMed: 8987733]

Diaz F, Villena A, Gonzalez P, Requena V, Rius F, Perez De Vargas I. Stereological age-related changes in neurons of the rat dorsal lateral geniculate nucleus. Anat Rec. 1999; 255:396–400. [PubMed: 10409812]

Dvorák K, Feit J. Migration of neuroblasts through partial necrosis of the cerebral cortex in newborn rats: contribution to the problems of morphological development and developmental period of cerebral microgyria. Acta Neuropathol. 1977; 38:203–212. [PubMed: 899721]

Dvorák K, Feit J, Juránková Z. Experimentally induced focal microgyria and status verrucosus deformis in rats: Pathogenesis and interrelation histological and autoradiographical study. Acta Neuropathol. 1978; 44:121–129. [PubMed: 716839]

Ferrer I, Alcántara S, Catala I, Zujar MJ. Experimentally induced laminar necrosis, status verrucosus, focal cortical dysplasia reminiscent of microgyria, and porencephaly in the rat. Exp Brain Res. 1993; 94:261–269. [PubMed: 8359242]

Ferrer I, Fabregues I, Palacios G. An autoradiographic study of methyl-azoxy-methanol acetate-induced cortical malformation. Acta Neuropathol. 1982; 57:313–315. [PubMed: 7136511]

Fitch RH, Brown CP, Tallal P, Rosen GD. Effects of sex and MK-801 on auditory-processing deficits associated with developmental microgyric lesions in rats. Behav Neurosci. 1997a; 111:404–412. [PubMed: 9106679]

Fitch RH, Miller S, Tallal P. Neurobiology of speech perception. Ann Rev Neurosci. 1997b; 20:331–353. [PubMed: 9056717]

Fitch RH, Tallal P, Brown C, Galaburda AM, Rosen GD. Induced microgyria and auditory temporal processing in rats: A model for language impairment? Cereb Cortex. 1994; 4:260–270. [PubMed: 8075531]

Galaburda AM, Kemper TL. Cytoarchitectonic abnormalities in developmental dyslexia; a case study. Ann Neurol. 1979; 6:94–100. [PubMed: 496415]

Galaburda AM, Menard MT, Rosen GD. Evidence for aberrant auditory anatomy in developmental dyslexia. Proc Natl Acad Sci U S A. 1994; 91:8010–8013. [PubMed: 8058748]

Galaburda AM, Sherman GF, Rosen GD, Aboitiz F, Geschwind N. Developmental dyslexia: Four consecutive cases with cortical anomalies. Ann Neurol. 1985; 18:222–233. [PubMed: 4037763]

Gardella D, Hatton WJ, Rind HB, Rosen GD, von Bartheld CS. Differential tissue shrinkage and compression in the z-axis: implications for optical disector counting in vibratome-, plastic- and cryosections. J Neurosci Methods. 2003; 124:45–59. [PubMed: 12648764]

Gavrieli Y, Sherman Y, Ben-Sasson SA. Identification of programmed cell death in situ via specific labeling of nuclear DNA fragmentation. J Cell Biol. 1992; 119:493–501. [PubMed: 1400587]

Giannetti S, Gaglini P, Di Rocco F, Di Rocco C, Granato A. Organization of cortico-cortical associative projections in a rat model of microgyria. Neuroreport. 2000; 11:2185–2189. [PubMed: 10923667]

Giannetti S, Gaglini P, Granato A, Di Rocco C. Organization of callosal connections in rats with experimentally induced microgyria. Childs Nerv Syst. 1999; 15:444–448. discussion 449–450. [PubMed: 10502002]

Goffinet AM. Events governing organization of postmigratory neurons: Studies on brain development in normal and reeler mice. Brain Res Rev. 1984; 7:261–296.

Gundersen HJ, Bagger P, Bendtsen TF, Evans SM, Korbo L, Marcussen N, Moller A, Nielsen K, Nyengaard JR, Pakkenberg B, et al. The new stereological tools: disector, fractionator, nucleator and point sampled intercepts and their use in pathological research and diagnosis. Apmis. 1988; 96:857–881. [PubMed: 3056461]

Gundersen HJG. Stereology of arbitrary particles. A review of unbiased number and size estimators and the presentation of some new ones, in memory of William R. Thompson. J Microsc. 1986; 143:3–45. [PubMed: 3761363]

Herman AE, Galaburda AM, Fitch HR, Carter AR, Rosen GD. Cerebral microgyria, thalamic cell size and auditory temporal processing in male and female rats. Cereb Cortex. 1997; 7:453–464. [PubMed: 9261574]

Hindmarsh GJ, O'Callaghan MJ, Mohay HA, Rogers YM. Gender differences in cognitive abilities at 2 years in ELBW infants. Extremely low birth weight. Early Hum Dev. 2000; 60:115–122. [PubMed: 11121674]

Humphreys P, Rosen GD, Press DM, Sherman GF, Galaburda AM. Freezing lesions of the newborn rat brain: A model for cerebrocortical microgyria. J Neuropath Exp Neurol. 1991; 50:145–160. [PubMed: 2010774]

Jacobs KM, Graber KD, Kharazia VN, Parada I, Prince DA. Postlesional epilepsy: the ultimate brain plasticity. Epilepsia. 2000; 41:S153–S161. [PubMed: 10999537]

Jacobs KM, Gutnick MJ, Prince DA. Hyperexcitability in a model of cortical maldevelopment. Cereb Cortex. 1996; 6:514–523. [PubMed: 8670677]

Jacobs KM, Kharazia VN, Prince DA. Mechanisms underlying epileptogenesis in cortical malformations. Epilepsy Res. 1999a; 36:165–188. [PubMed: 10515164]

Jacobs KM, Mogensen M, Warren E, Prince DA. Experimental microgyri disrupt the barrel field pattern in rat somatosensory cortex. Cereb Cortex. 1999b; 9:733–744. [PubMed: 10554996]

Jacobs KM, Prince DA. Excitatory and inhibitory postsynaptic currents in a rat model of epileptogenic microgyria. J Neurophysiol. 2005; 93:687–696. [PubMed: 15385597]

Kulesza RJ, Vinuela A, Saldana E, Berrebi AS. Unbiased stereological estimates of neuron number in subcortical auditory nuclei of the rat. Hear Res. 2002; 168:12–24. [PubMed: 12117505]

Lauterbach MD, Raz S, Sander CJ. Neonatal hypoxic risk in preterm birth infants: the influence of sex and severity of respiratory distress on cognitive recovery. Neuropsychology. 2001; 15:411–420. [PubMed: 11499996]

Lee KS, Schottler F, Collins JL, Lanzino G, Couture D, Rao A, Hiramatsu K, Goto Y, Hong SC, Caner H, Yamamoto H, Chen ZF, Bertram E, Berr S, Omary R, Scrable H, Jackson T, Goble J, Eisenman L. A genetic animal model of human neocortical heterotopia associated with seizures. J Neurosci. 1997; 17:6236–6242. [PubMed: 9236234]

Livingstone M, Rosen G, Drislane F, Galaburda A. Physiological and anatomical evidence for a magnocellular defect in developmental dyslexia. Proc Natl Acad Sci U S A. 1991; 88:7943–7947. [PubMed: 1896444]

Luczynska A, Dziewiatkowski J, Jagalska-Majewska H, Kowianski P, Wojcik S, Labuda C, Morys J. Qualitative and quantitative analysis of the postnatal development of the ventroposterolateral nucleus of the thalamus in rat and rabbit. Folia Morphol (Warsz). 2003; 62:75–87. [PubMed: 12866666]

Luhmann HJ, Raabe K. Characterization of neuronal migration disorders in neocortical structures. 1. Expression of epileptiform activity in an animal model. Epilepsy Res. 1996; 26:67–74. [PubMed: 8985688]

Luhmann HJ, Raabe K, Qü M, Zilles K. Characterization of neuronal migration disorders in neocortical structures: extracellular *in vitro* recordings. Eur J Neurosci. 1998; 10:3085–3094. [PubMed: 9786203]

Marret S, Mukendi R, Gadisseux J, Gressens P, Evrard P. Effect of ibotenate on brain development: An excitotoxic mouse model of microgyria and postthypoxic-like lesions. J Neuropathol Exp Neurol. 1995; 54:358–370. [PubMed: 7745435]

Meencke HJ, Janz D. Neuropathological findings in primary generalized epilepsy: a study of eight cases. Epilepsia. 1984; 25:8–21. [PubMed: 6692795]

Nicolelis MAL, Chapin JK, Lin RCS. Neonatal whisker removal in rats stabilizes a transient projection from the auditory thalamus to the primary somatosensory cortex. Brain Res. 1991; 567:133–139. [PubMed: 1726139]

Palmini A, Andermann F, Olivier A, Tampieri D, Robitaille Y, Andermann E, Wright G. Focal neuronal migration disorders and intractable partial epilepsy: A study of 30 patients. Ann Neurol. 1991a; 30:741–749. [PubMed: 1789691]

Palmini A, Andermann F, Olivier A, Tampieri D, Robitaille Y, Melanson D, Ethier R. Neuronal migration disorders: A contribution of modern neuroimaging to the etiologic diagnosis of epilepsy. Can J Neurol Sci. 1991b; 18:580–587. [PubMed: 1777874]

Paxinos, G.; Watson, C. The rat brain in stereotaxic coordinates. Sydney: Academic Press; 1986.

Peiffer AM, Dunleavy CK, Frenkel M, Gabel LA, LoTurco JJ, Rosen GD, Fitch RH. Impaired detection of variable duration embedded tones in ectopic NZB/BINJ mice. Neuroreport. 2001; 12:2875–2879. [PubMed: 11588594]

Peiffer AM, Fitch RH, Thomas JJ, Yurkovic AN, Rosen GD. Brain weight differences associated with induced focal microgyria. BMC Neurosci. 2003; 4:12. [PubMed: 12823865]

Peiffer AM, Rosen GD, Fitch RH. Rapid auditory processing and MGN morphology in microgyric rats reared in varied acoustic environments. Brain Res Dev Brain Res. 2002; 138:187–193.

Peiffer AM, Rosen GD, Fitch RH. Sex differences in rapid auditory processing deficits in microgyric rats. Brain Res Dev Brain Res. 2004; 148:53–57.

Raz N, Torres IJ, Acker JD. Age, gender, and hemispheric differences in human striatum: a quantitative review and new data from in vivo mRI morphometry. Neurobiol Learn Mem. 1995; 63:133–142. [PubMed: 7663886]

Rice DS, Sheldon M, D'Arcangelo G, Nakajima K, Goldowitz D, Curran T. Disabled-1 acts downstream of Reelin in a signaling pathway that controls laminar organization in the mammalian brain. Development. 1998; 125:3719–3729. [PubMed: 9716537]

Rosen GD, Burstein D, Galaburda AM. Changes in efferent and afferent connectivity in rats with cerebrocortical microgyria. J Comp Neurol. 2000; 418:423–440. [PubMed: 10713571]

Rosen GD, Galaburda AM. Single cause, polymorphic neuronal migration disorders: an animal model. Dev Med Child Neurol. 2000; 42:652–662. [PubMed: 11085292]

Rosen GD, Harry JD. Brain volume estimation from serial section measurements: a comparison of methodologies. J Neurosci Methods. 1990; 35:115–124. [PubMed: 2283883]

Rosen GD, Herman AE, Galaburda AM. MGN neuronal size distribution following induced neocortical malformations: The effect of perinatal gonadal steroids. Soc Neurosci Abstr. 1997; 23:626.

Rosen GD, Herman AE, Galaburda AM. Sex differences in the effects of early neocortical injury on neuronal size distribution of the medial geniculate nucleus in the rat are mediated by perinatal gonadal steroids. Cereb Cortex. 1999; 9:27–34. [PubMed: 10022493]

Rosen GD, Press DM, Sherman GF, Galaburda AM. The development of induced cerebrocortical microgyria in the rat. J Neuropathol Exp Neurol. 1992a; 51:601–611. [PubMed: 1484290]

Rosen GD, Sherman GF, Richman JM, Stone LV, Galaburda AM. Induction of molecular layer ectopias by puncture wounds in newborn rats and mice. Dev Brain Res. 1992b; 67:285–291. [PubMed: 1380903]

Rosen GD, Windzio H, Galaburda AM. Unilateral induced neocortical malformation and the formation of ipsilateral and contralateral barrel fields. Neuroscience. 2001; 103:931–939. [PubMed: 11301202]

Schmued LC, Albertson C, Slikker W Jr. Fluoro-Jade: a novel fluorochrome for the sensitive and reliable histochemical localization of neuronal degeneration. Brain Res. 1997; 751:37–46. [PubMed: 9098566]

Sweet HO, Bronson RT, Johnson KR, Cook SA, Davisson MT. Scrambler, a new neurological mutation of the mouse with abnormalities of neuronal migration. Mamm Genome. 1996; 7:798–802. [PubMed: 8875886]

Tallal P, Piercy M. Developmental aphasia: rate of auditory processing and selective impairment of consonant perception. Neuropsychologia. 1974; 12:83–93. [PubMed: 4821193]

Williams RW, Rakic P. Three-dimensional counting: An accurate and direct method to estimate numbers of cells in sectioned material. J Comp Neurol. 1988; 278:344–352. [PubMed: 3216047]

Zilles, K. The cortex of the rat: a stereotaxic atlas. Berlin: Springer-Verlag; 1985.

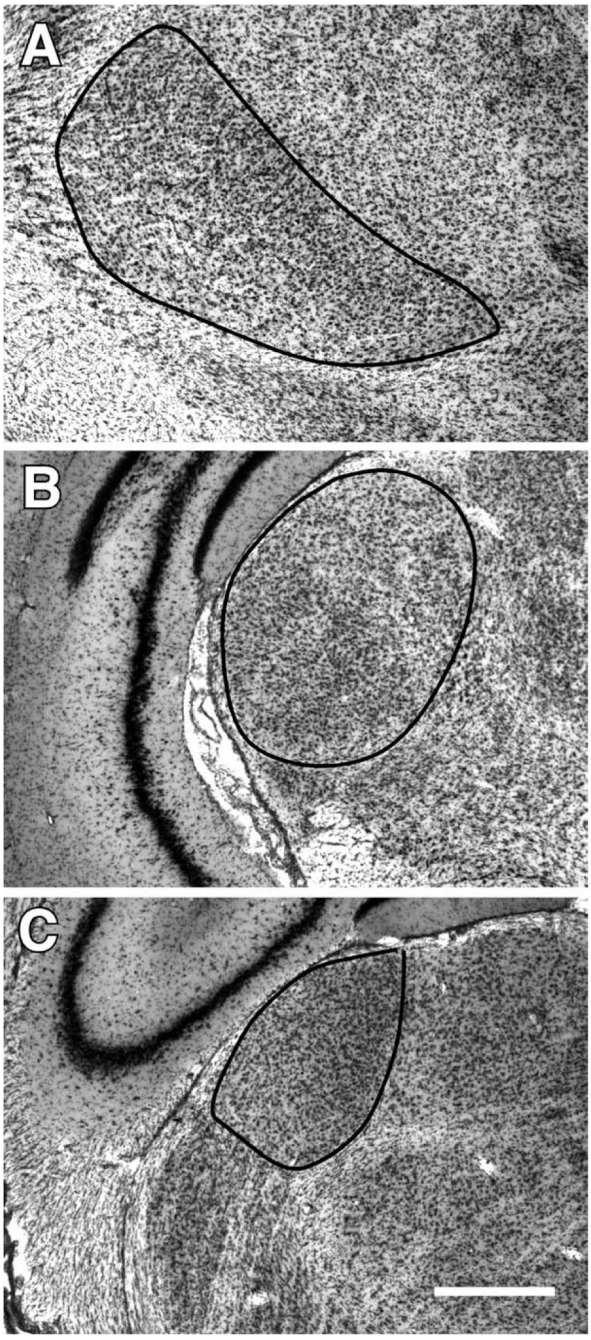

Fig. 1.
Delineation of the VB (A), the MGN (B), and the dLGN (C). Scale bar=500 μm.

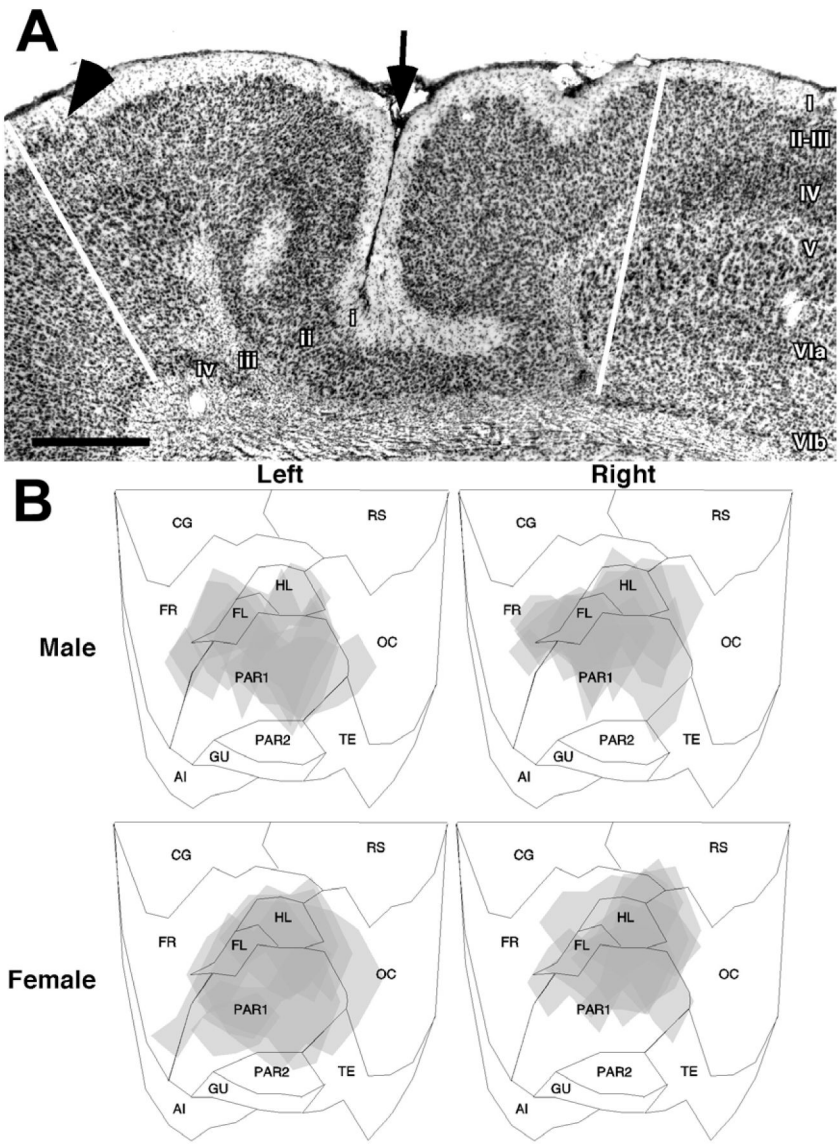

Fig. 2.

(A) Photomicrograph of a typical neocortical malformation following freezing injury to the developing cortical plate. In comparison to the normal six-layered cortex (right), the malformation consists of a sulcus (arrow), and four layers. Layer i is contiguous with the molecular layer. Layer ii is contiguous with layers II–III of the intact neocortex. Layer iii is the lamina dissecans, and consists of the remnants of the cortical plate that is damaged by the freezing injury. Layer iv, when present, is contiguous with the subplate (layer VIb). Arrowhead indicates a layer ii dysplasia. Scale bar=500 μm. The lower half of the figure is flattened maps of the neocortex illustrating regions of damage of the left and right hemisphere of male and female rats used in the experiment 1.

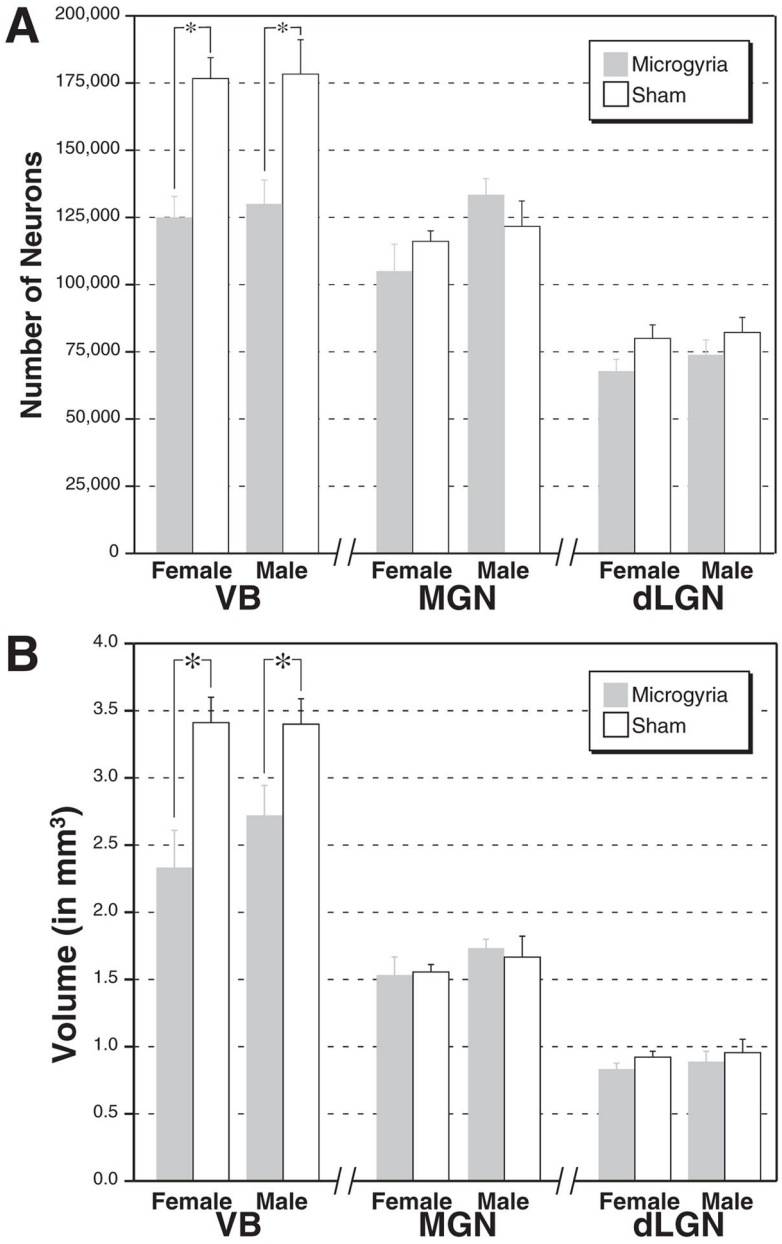

Fig. 3.

(A) Mean (±S.E.M.) number of neurons in the VB, MGN, and dLGN nuclei of the thalamus in male and female rats either with microgyria (dark bars) or shams (white bars). In VB, both male and female subjects with microgyria have significantly fewer neurons than their sham counterparts. There are no significant differences in neuron number in other thalamic nuclei. (B) Mean (±S.E.M.) volume of thalamic nuclei in subjects with and without induced malformations of the somatosensory neocortex. The volume of VB is significantly decreased in both male and female subjects with microgyria (dark bars) when compared with shams (white bars). There are no significant differences in volume in MGN or dLGN.

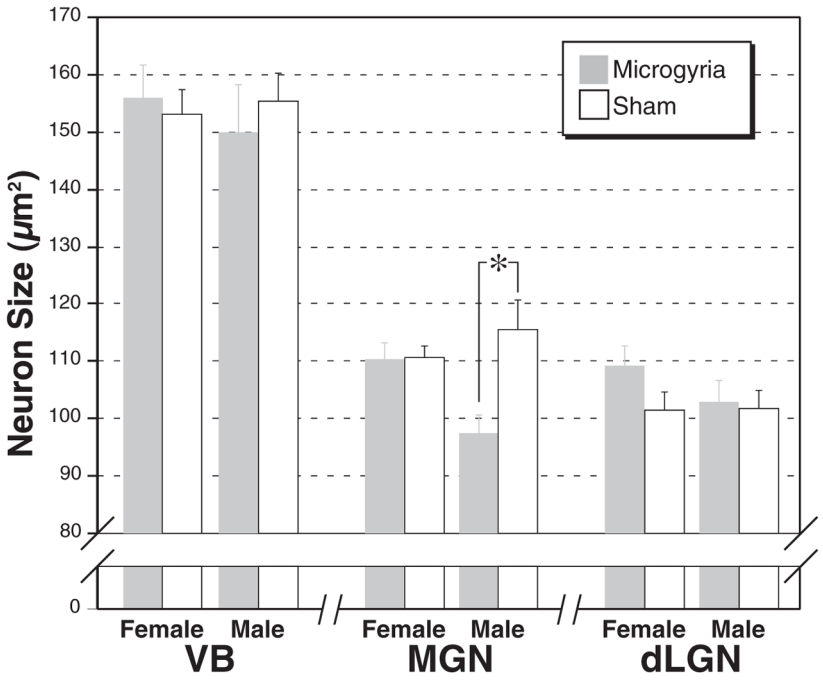

Fig. 4.

Mean (±S.E.M.) neuron size in VB, MGN, and dLGN of male and female subjects either with (dark bars) or without (white bars) microgyria. The size of neurons in male subjects with microgyria is significantly smaller in MGN.

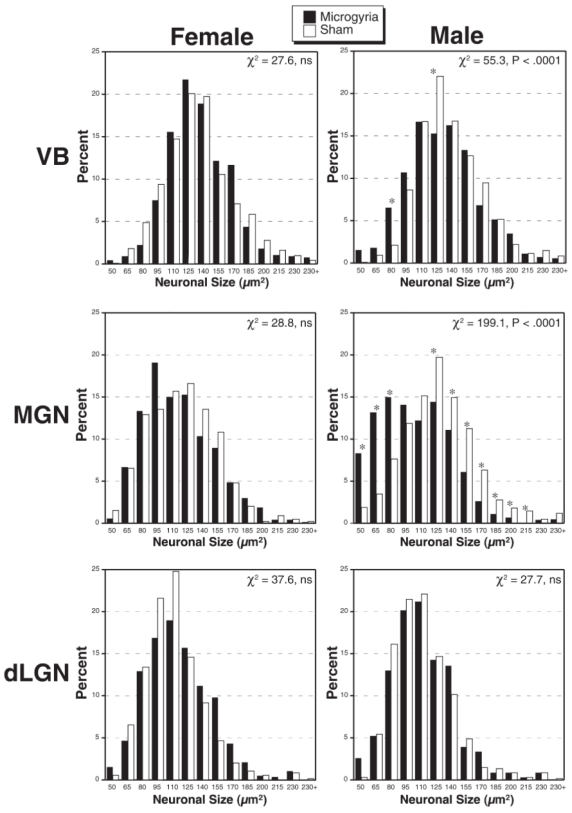

Fig. 5.

Frequency histograms of neuronal size in lesioned (black) and sham (white) male and female subjects. In VB and MGN there is a significant difference in distribution of cell sizes in males, with there being more small and fewer large neurons in subjects with microgyria. There are no significant differences in cell size distribution in the dLGN. Asterisks indicate bins with significant contributions to the chi-square.

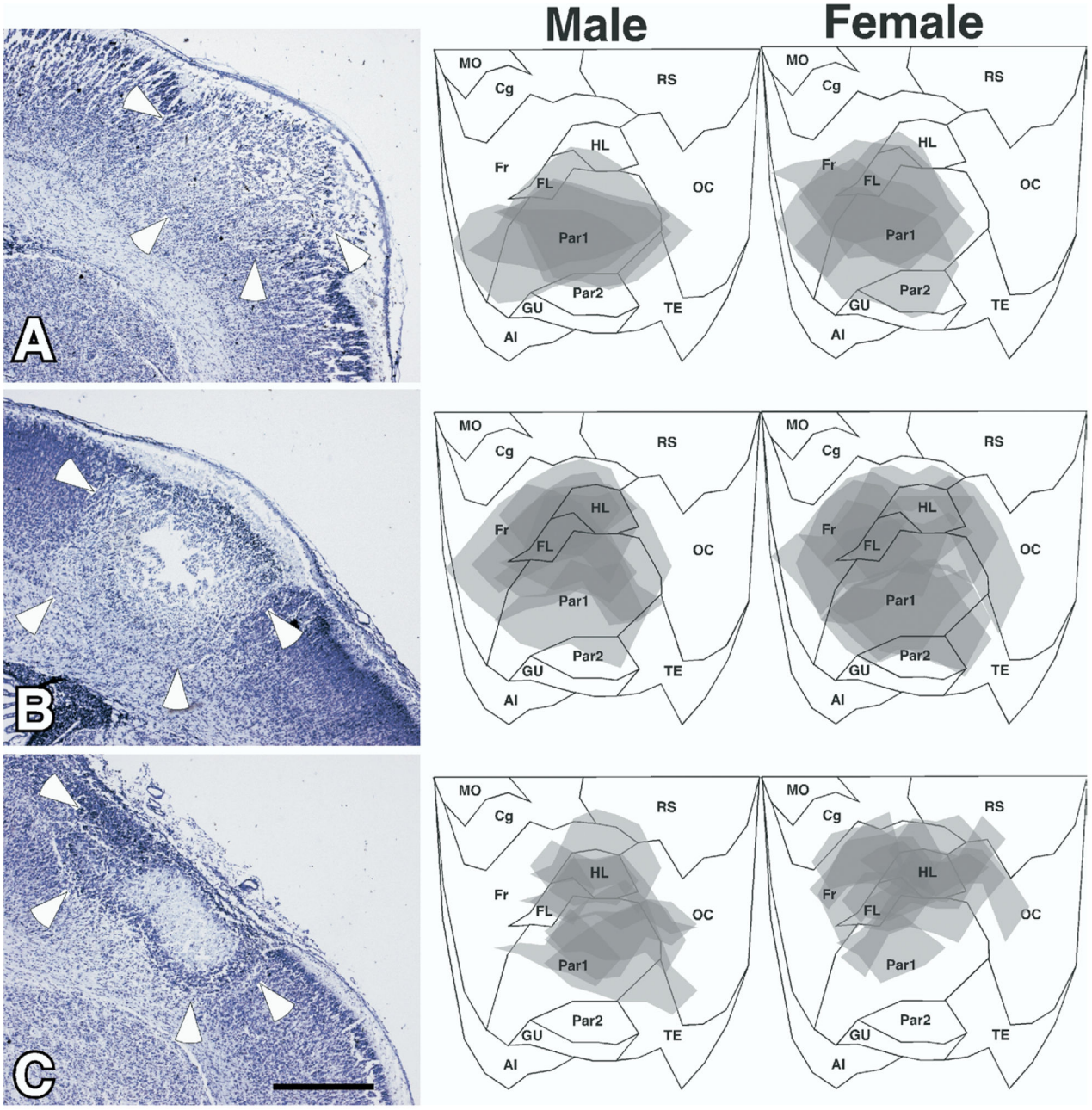

Fig. 6.

Photomicrograph of freezing lesion and flattened map of lesion location for 8 h (panel A), 24 h (panel B), and 72 h (panel C) subjects. Arrowheads indicate border of lesioned area. Scale bar=500 μm.

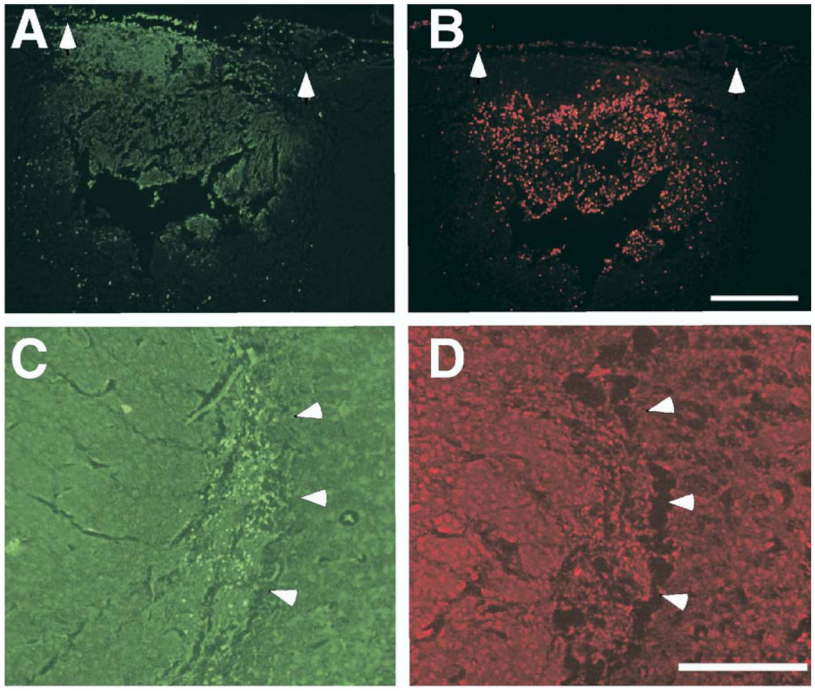

Fig. 7.

Fluorescence photomicrographs of FJB-positive and TUNEL-positive profiles. (A) FJB-stained profiles in a lesioned area of the neocortex (arrowheads define medial and lateral border). (B) Section adjacent to panel A stained for TUNEL (arrowheads define medial and lateral border). (C) FJB positive profiles in the VB nucleus of the thalamus (arrowheads define lateral border). (D) Section adjacent to panel C stained for TUNEL (arrowheads aligned with panel C). Scale bar=250 μm.

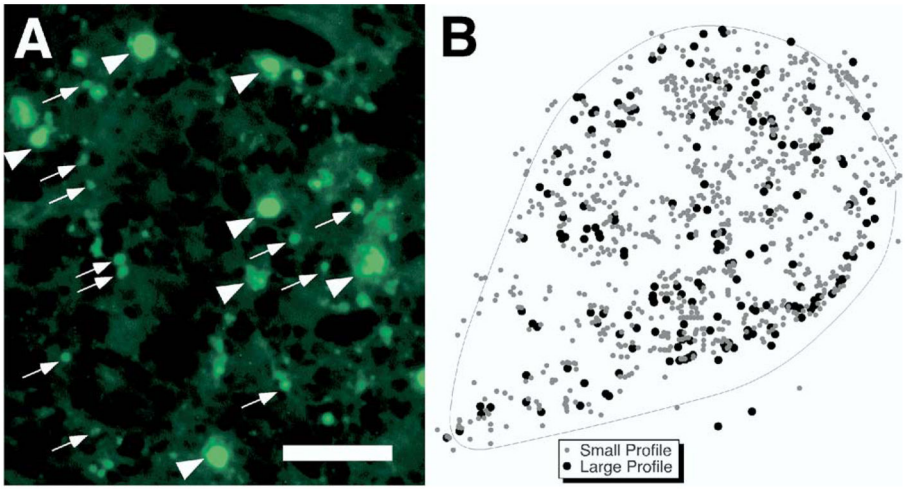

Fig. 8.

(A) FJB-stained profiles in VB. Arrowheads denote large profiles, while arrows denote small profiles. Scale bar=25 μm. (B) Tracing from neurolucida of large (black circles) and small (gray circles) profiles in VB from one section.

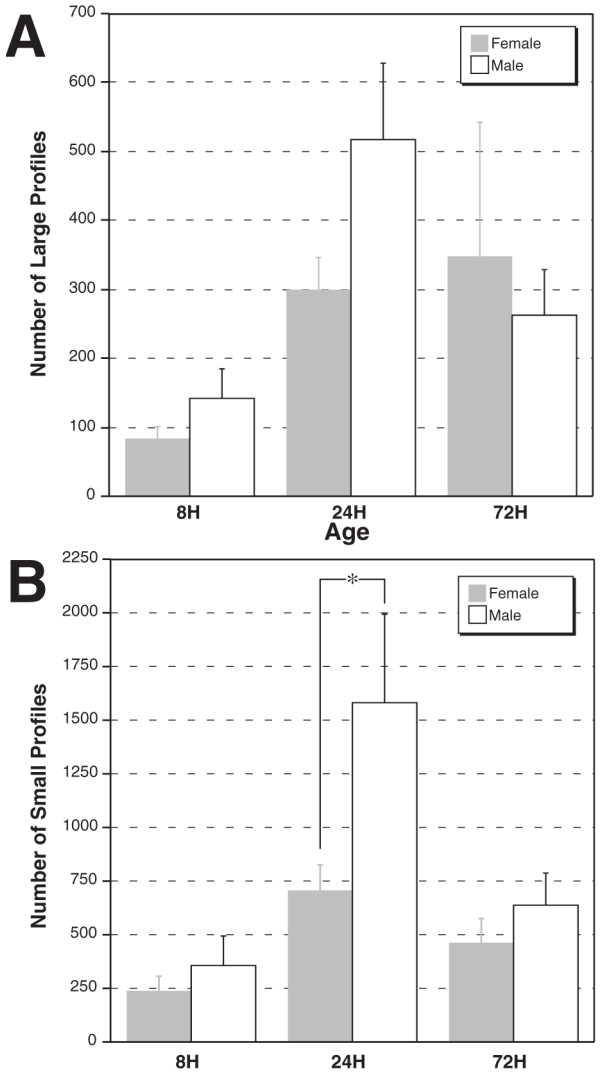

Fig. 9.

Mean (±S.E.M.) number of large and small profiles in VB of female (dark bars) and male (white bars) subjects with microgyria. (A) There were no significant differences in large profiles. (B) There are significant main effects of Sex and Age in the number of small profiles, with an increased number of profiles in the 24 h group. There is a sex difference at this age with females having fewer profiles than males.

Table 1

Parameters for stereologic probes for experiment 1

Thalamic nuclei	Optical fractionator and nucleator			Point counting, sampling frequency (μm)	Section periodicity
	Counting frame (μm)	Disector height	Sampling frequency (μm)		
VB	30×30	20	250×250	250×250	Every 10th
MGN	25×25	20	250×250	250×250	Every 5th
dLGN	25×25	20	225×225	200×200	Every 5th

Table 2

Subjects in experiment 2

Group	Duration	Age	*N*	
			Male	Female
Microgyria	5	8	4	4
Microgyria	5	24	7	9
Microgyria	10	24	2	2
Microgyria	5	72	9	6
Microgyria	10	72	4	6
Microgyria	5	120	2	2
Microgyria	5	168	4	4
Summary			32	33
Sham	5 s	24	1	3
Sham	5 s	72	3	1
Summary			4	4

Table 3

FJB-positive profiles in VB

	Microgyria		Sham	
	Female	**Male**	**Female**	**Male**
Large profiles	287.7±79.5	332.4±57.4	43.0±7.2	46.0±5.8
Small profiles	537.1±76.2	918.5±179.9	33.5±14.2	24.8±3.8

Values are means±SEM.